Physics of Fluids

LETTER | MAY 11 2022

Study of preferential concentration in turbulent flows using combined graph theory and Voronoï analysis

Paul Andrade ; Yannis Hardalupas; Georgios Charalampous

Check for updates

Physics of Fluids 34, 051704 (2022)
https://doi.org/10.1063/5.0091469

View Online
Export Citation

26 March 2024 16:31:13


APL Energy
Latest Articles Online!
Read Now
AIP Publishing

AIP Publishing

Physics of Fluids LETTER scitation.org/journal/phf

Study of preferential concentration in turbulent flows using combined graph theory and Voronoï analysis

Cite as: Phys. Fluids **34**, 051704 (2022); doi: 10.1063/5.0091469
Submitted: 15 March 2022 · Accepted: 25 April 2022 ·
Published Online: 11 May 2022

View Online Export Citation CrossMark

Paul Andrade,[1] Yannis Hardalupas,[1] and Georgios Charalampous[2,a)]

AFFILIATIONS

[1]Mechanical Engineering Department, Imperial College London, London, United Kingdom
[2]Mechanical Engineering Department, University of Thessaly, Volos, Greece

[a)]Author to whom correspondence should be addressed: georgios.charalampous@uth.gr

ABSTRACT

Collisions between particles in turbulent flows may be enhanced by the formation of clusters due to the preferential concentration effect. However, the internal sub-structure of the clusters remains unclear. This paper describes using the "degree of a node" and the "shortest path length" from graph theory, in combination with Voronoï analysis, to gain further insight into both the structure and internal sub-structure of a cluster. This is demonstrated on experimental measurements obtained from a confined counter-flow/jet system. A minority of the particles, which comprise large clusters, are found to have a significantly large number of neighboring particles for collisions. However, particles which comprise small clusters typically have a random number of neighbors.

Published under an exclusive license by AIP Publishing. https://doi.org/10.1063/5.0091469

26 March 2024 16:31:13

Solid or liquid particles dispersed in turbulent flows are found in many natural and industrial processes such as cloud physics and spray drying.[1,2] Under certain flow conditions, an interesting peculiarity of these flows is the tendency of the particles to disperse in a nonrandom way, due to interactions between particles and surrounding turbulent fluctuations. This leads to regions in space where there exists a significantly higher concentration of particles than the mean concentration, called "clusters." In addition, there also exist regions where there is a very low concentration of particles than the mean, called "voids." This effect is commonly referred to as preferential concentration and is most pronounced when an appropriate Stokes number, St_F, which characterizes the interaction between the particles and the local flow eddies, is of the order of unity.[3,4]

The preferential concentration effect is believed to enhance the probability of collisions, which may occur in the flow.[5] The collision of particles in turbulent gas flows is often an important feature in the processes described above, specifically in the formation of rain (cloud physics) and agglomeration (spray drying). Several methodologies have therefore been used to gain insight into the preferential concentration effect and, in particular, obtain statistical information about the structure of the clusters which form. Some of these methods include "box counting," "Voronoï analysis," "skeletonization,"[6–8] and "the radial distribution function."[5]

The box counting method, described in Ref. 6, partitions an image of particles into small rectangular boxes, and the number of particles in each box, denoted $\mathcal{N}_P$, is counted. Let σ represent the standard deviation of the set of values of $\mathcal{N}_P$ for the image of particles. Let σ_P represent the standard deviation of the set of values of $\mathcal{N}_P$ for the idealized case where the same number of particles is instead distributed randomly in space. A nondimensional number, D, uses this information to characterize the extent of the preferential concentration effect observed in the image, where $D = \frac{\sigma - \sigma_P}{\gamma}$. Here, γ is the mean particle number density, that is, the total number of particles divided by the total number of boxes. If $D > 0$, then clusters are present in the image. If $D \to 0$, the particles in the image are distributed in space in a random way. If $D < 0$, the particles are distributed in an ordered manner. The box counting method also provides a simple way to determine a characteristic length scale of the clusters. This corresponds to the length of the box used to partition the image. However, determining the size of the box, which best partitions the image to observe the preferential behavior, is not always simple. Also, since each box has the same shape and size, it is not possible to identify accurately individual clusters in the image. This is because a cluster may have a wide range of different shapes and sizes and therefore cannot be described with an integer number of boxes of the same shape and size. The radial distribution function quantifies particle density as a

Published under an exclusive license by AIP Publishing

function of distance from a central particle. As such, it averages out information across the investigated domain and does not provide information on individual clusters.

The Voronoï analysis method, proposed in Ref. 7, is in many ways an improvement to box counting. It can also be used to quantify the extent of the preferential concentration effect. In addition, it is possible to identify individual clusters. A 2D image of particles is partitioned into "Voronoï cells," where each cell contains one and only one particle. It follows that for all points within each cell, the distance to the particle enclosed by the cell is shorter than the distance to any particle outside the cell. The shape and size of each Voronoï cell is determined by the position of all the particles in the image. In a small neighborhood, if the particles are close together, the Voronoï cells in that region must be very small in size in accordance with the definition that each cell can contain only one particle. The size of the i th Voronoï cell is characterized in two dimensions by its area, $\mathcal{A}_i$. Therefore, if the area of the Voronoï cells in a small neighborhood is found to reduce in size, the concentration of particles in that neighborhood must have increased. The standard deviation of the set of all normalized Voronoï cell areas, $\mathcal{A}_i/\langle\mathcal{A}\rangle$, is denoted $\sigma_{\mathcal{A}}$, where $\langle\mathcal{A}\rangle$ is the mean area of all the Voronoï cells in the image. The standard deviation of the set of all normalized Voronoï cell areas for the case where the particles are distributed randomly in space is denoted $\sigma_{\mathcal{A}_p}$. Using an analytical fit from simulated data,[9] it is estimated that $\sigma_{\mathcal{A}_p} \approx 0.53$.[7] If $\sigma_{\mathcal{A}} > 0.53$, clusters are present in the flow. If $\sigma_{\mathcal{A}} \sim 0.53$, the particles are distributed randomly in space. Alternatively, if $\sigma_{\mathcal{A}} < 0.53$, the particles are distributed in an ordered way. Individual clusters are identified by assuming that Voronoï cells below a threshold for the area, τ, may comprise a cluster. The threshold used for the area is determined by the point of intersection on the left tail of two probability density functions (PDFs). These two functions describe $\mathcal{A}_i/\langle\mathcal{A}\rangle$ for the result obtained from the image domain and the case where the particles are distributed randomly in space. Suppose $\mathcal{Z}_\mathrm{i}$ corresponds to a Voronoï cell, which is below the threshold τ. An adjacency matrix is constructed to determine the connectivity between the set of $\mathcal{Z}_\mathrm{i}$. In other words, a cluster is identified when several Voronoï cells, which fall below a certain size, denoted by $\mathcal{Z}_\mathrm{i}$, share a common boundary. The structure of the cluster such as its area and perimeter, as well as its orientation, may then be determined. The technique can also be applied in three dimensions using Voronoï cells characterized instead by their volume. The main drawback to the Voronoï technique is that it does not provide a direct means to obtain a characteristic length scale of the clusters.

Skeletonization is an image analysis technique used to simplify a 2D object into a simpler "skeleton" object containing a series of lines, which together retain the main features of the original object. This is analogous to drawing a stick figure to represent the human body. The method may require image filtering and also pruning, where certain lines are removed to ensure the remaining skeleton only contains what are considered to be the most important lines. The method was recently used[8] to identify cluster objects in dense multiphase flows. The advantage of the method is that it allows the possibility of obtaining a characteristic length scale of the clusters. However, it is not always clear what are the important lines to retain.

Despite the use of the methods described above, little is known about how the sub-structure of a particular cluster can promote collisions. For example, it may be desirable to have particle clusters which span a large area since these clusters may contain more particles.[10] However, large clusters may be elongated in appearance, and therefore, many of the particles in such a cluster may not be in close proximity for a collision to occur. Smaller clusters in comparison may contain fewer particles, but the collision probability may be higher because the particles may be in close proximity due to the more rounded cluster shape. The purpose of this study is to put forward the idea of using graph theory, after using the Voronoï analysis technique, to give insight into this issue. It will also be shown that graph theory can be used to obtain an approximate skeleton-like structure of a cluster identified from the Voronoï analysis, therefore providing a means to estimate its characteristic length scale.

Graphs are a mathematical diagram, which represent interactions between collections of objects. The objects are represented as nodes, and the interaction between the objects are represented as edges, which connect to adjacent nodes. A simple graph is one where the interaction between any two adjacent nodes is represented using one and only one edge and a node cannot interact with itself (where such an edge is called a loop). Otherwise, the graph is said to be a multigraph. Examples of simple graphs and multigraphs are shown in Fig. 1. A path is the edges traversed to go from one node to another node in the graph, without visiting the same node twice.

A graph is described as unweighted if the strength of the interaction for each edge is the same. On the other hand, if the graph is weighted, each edge is associated with a weight, which signifies the strength of the interaction for that particular edge and its node(s). A graph is connected if for all nodes, there exists an edge path to all other nodes. A graph is described as regular if each node has the same number of edges, which are connected to it. A complete graph is one where all nodes are directly connected to each other by a single edge.

Now consider a single cluster, $\mathcal{C}_k$ of N-Voronoï cells, that is, $\mathcal{Z}_1, \ldots, \mathcal{Z}_\mathrm{N}$. Let the symbol $\mathcal{G}$ denote a graph where all particles of cluster $\mathcal{C}_k$ constitute its nodes. Each Voronoï cell, $\mathcal{Z}_\mathrm{i}$, is associated with a single node, x_i. The set of all nodes is referred to as V. An edge of a graph, $e_{\mathrm{i,j}}$, is defined whereby two Voronoï cells $\mathcal{Z}_\mathrm{i}$ and $\mathcal{Z}_\mathrm{j}$ share a common boundary. The shared part of the boundary between the i th and j th cell is denoted $\mathcal{B}_{\mathrm{i,j}}$ (Fig. 2). In other words, an edge exists if two Voronoï cells, $\mathcal{Z}_\mathrm{i}$ and $\mathcal{Z}_\mathrm{j}$, are directly connected to each other. The set of all edges is referred to as E. A graph that represents the cluster is therefore $G_\mathcal{C} = (V, E)$. An example of a cluster obtained using Voronoï analysis and its associated representation as an unweighted graph is shown in Fig. 2. The figure shows only a portion of the cluster and graph for clarity. Note that there are many different ways to visualize the cluster and they are morphologically the same, as long as they share the same nodes and edge interactions.

Let $d_{\mathrm{i,j}}$ represent the Euclidean distance between particle i and particle j, which reside in the cluster. If there exists an edge that connects node i and node j, then this edge can be assigned a weight, $w_{\mathrm{i,j}}$, as a function of distance. In this way, a simple weighted graph may be constructed, which accounts for distance between particles. The weight can be defined in many ways depending on the performed analysis. For unweighted simple graphs, the value of the weight for all edges is unity.

The graph $G_\mathcal{C}$ is computed directly for a given cluster, $\mathcal{C}_k$ by construction of a weighted adjacency matrix, A, as shown in Eq. (1).[11] This equation states that if two Voronoï cells $\mathcal{Z}_\mathrm{i}$ and $\mathcal{Z}_\mathrm{j}$ from the cluster $\mathcal{C}_k$ share a common boundary, the value in the i th row and j th

26 March 2024 16:31:13

Published under an exclusive license by AIP Publishing

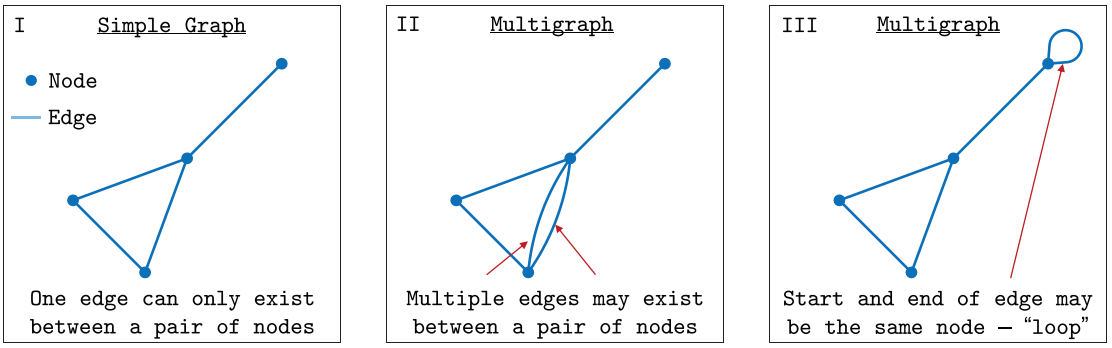


FIG. 1. Visualizations of several different graphs. Figure (I) is an example of a simple graph. Figures (II) and (III) are examples of multigraphs because they contain some combination of multiple edges between two nodes or loops.

column is given by the weight, $w_{i,j}(d_{i,j})$. Since $w_{i,j} = w_{j,i}$, A is a square symmetric matrix. If an element is along the diagonal of the matrix, which determines whether a boundary exists between a cell $\mathcal{Z}_i$ and itself, the value is given as zero (hollow matrix). All other elements in the adjacency matrix have the value of zero, as no boundaries are shared between the respective cells

$$A_{i,j} = \begin{cases} w_{i,j}, & \text{if } i \neq j \text{ and } \mathcal{Z}_i \& \mathcal{Z}_j \text{ share a boundary,} \\ 0, & \text{if } i = j \text{ (no loops),} \\ 0, & \text{otherwise (no shared boundary).} \end{cases} \quad (1)$$

Other matrices that are also used to characterize graphs include the degree matrix, D and the Laplacian matrix, L. These matrices and their properties are not explored in the present paper. The graphs associated with the clusters, as presented above, must have the following properties:

- The graphs are simple, since the connection between two Voronoï cells is represented by one and only one edge and a Voronoï cell cannot interact with itself.
- The graphs are connected, since all the Voronoï cells which comprise a given cluster, $\mathcal{Z}_1, \ldots, \mathcal{Z}_N$, are known to be connected to at least one other Voronoï cell.
- In general, the graphs are not regular nor complete. This is because Voronoï cells located at the periphery of a cluster may have a smaller neighborhood of surrounding cells than Voronoï cells found in the bulk of the cluster.

In this work, two tools from graph theory are utilized to supplement Voronoï analysis, which are the degree and the shortest path length. This is shown in the schematic in Fig. 3. In a unweighted graph, the degree of a node refers to the notion of counting the number of edges connected to that node. In this context, if an arbitrary Voronoï cell $\mathcal{Z}_i$ is chosen, the degree is then the number of neighboring cells connected to $\mathcal{Z}_i$. For example, in Fig. 2, the degree for $\mathcal{Z}_1$ is 2, and for $\mathcal{Z}_3$, it is 3. In a weighted graph, the degree of a node is the summation of the weights assigned to the edges, which are connected to it. A large degree for $\mathcal{Z}_i$ corresponds to particle i having a greater number of particles which neighbor it, which suggests that locally,

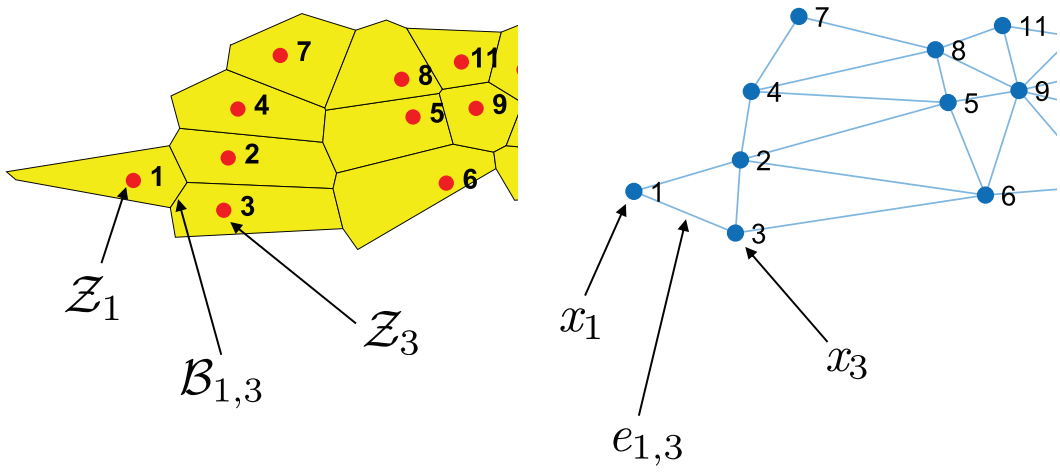


FIG. 2. Each cluster contains N-Voronoï cells, with each Voronoï cell in the cluster denoted by $\mathcal{Z}_1, \ldots, \mathcal{Z}_N$. Each Voronoï cell (or the particle which resides inside it) corresponds to node $x_1, \ldots, x_N$ on the graph. An edge on the graph, denoted by $e_{i,j}$, represents two Voronoï cells $\mathcal{Z}_i$ and $\mathcal{Z}_j$, which share part of their cell boundary. The figure shows the interaction between the Voronoï cells $\mathcal{Z}_1$ and $\mathcal{Z}_3$ and the corresponding representation as a graph.

26 March 2024 16:31:13

Published under an exclusive license by AIP Publishing

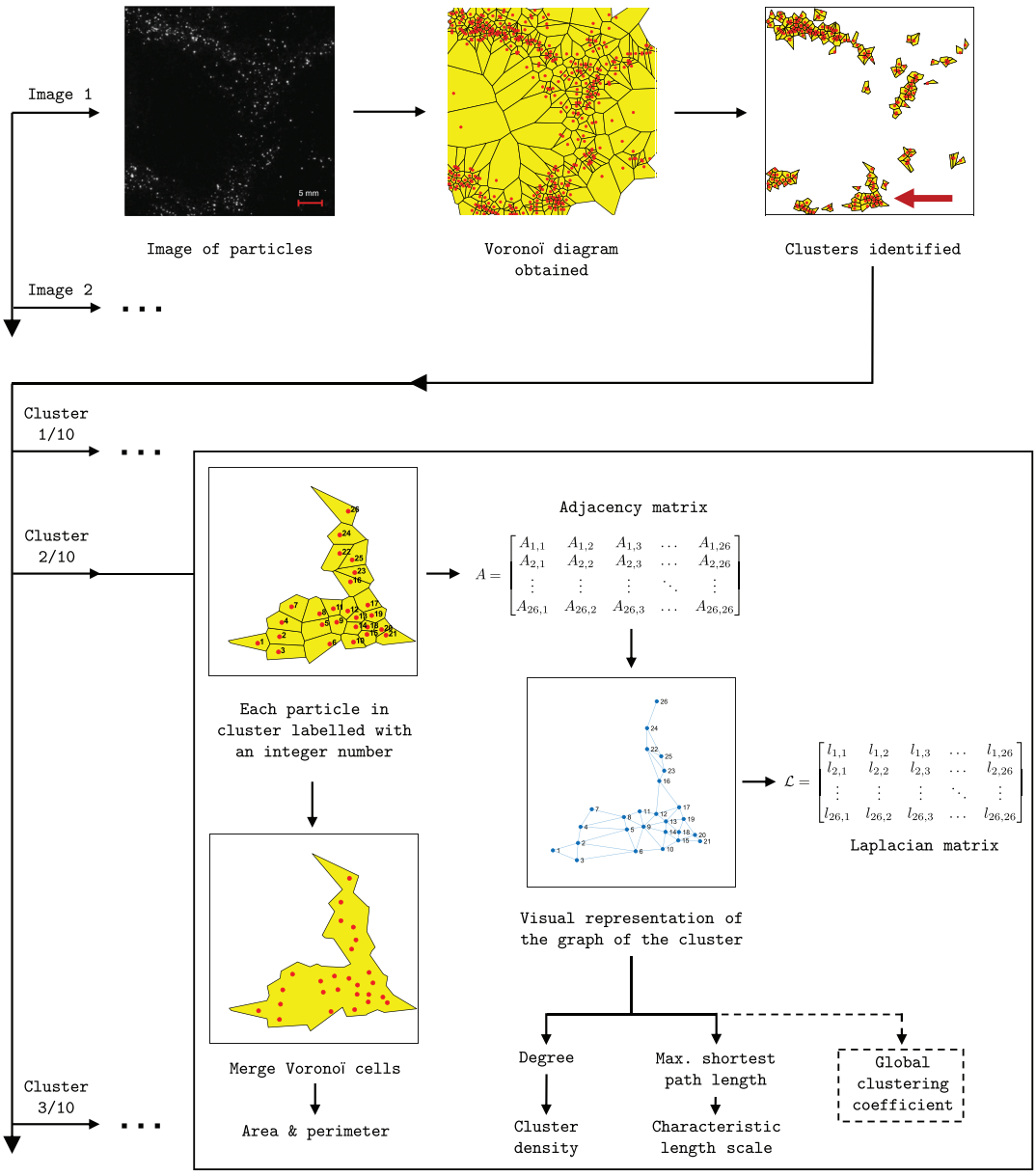


FIG. 3. Schematic of the Voronoï analysis and graph theory methodology to identify and characterize clusters of particles from an image. Parts in the dashed lines are additional tools, which may also give further insight. The experimental data used for the figure are obtained from a counter-flow/jet experiment system, which is described in further detail in the text.

there is a possibility that more collisions may occur. A distribution of the degree of all the nodes can then be obtained. A skewed distribution would suggest that locally within the cluster, there exist some particles, which could undergo a significantly higher or lower number of collisions than the mean. This may also suggest that the clusters have some sub-structure.

The shortest path length is the fewest number of edges it takes to get from one node of a graph to another. In Fig. 2 on the graph, there are several ways to get from node 5 to node 1. One path goes from node 5 to node 6, then to node 3 and finally to node 1. However, the path that uses the fewest edges is the path from node 5 to node 2 and then to node 1. Since the graph is connected, a shortest path length can be found between any pair of Voronoï cells, $\mathcal{Z}_i$ and $\mathcal{Z}_j$. Suppose each edge in the graph is weighted by the distance between the particles. Then, an approximate skeleton can be constructed between any pair of Voronoï cells, more specifically the particles, which reside in

26 March 2024 16:31:13

Published under an exclusive license by AIP Publishing

those cells, by traversing all the edges along the shortest path. The maximum shortest path may then be considered as a characteristic length scale of the cluster, since it expresses the minimum distance traversing along edges between the two remotest particles in the cluster. Its length is obtained by summation of the distances with which each edge in the path is associated. An example of this is shown in Fig. 4. This avoids the need to carry out a skeletonization, which typically requires some form of image filtering.[8] It also avoids a bounding box approach or area equivalent circle,[12] which may not accurately represent the cluster shape.

In brief, the Voronoï analysis provides information about the extent of the clustering, identification of individual clusters, and external structure of each cluster (such as area and perimeter). Graph theory additionally provides further external structure (characteristic length scale) and internal structure (neighboring particle distribution). While graph theory is not limited by Reynolds or Stokes numbers directly, it is limited to dilute flows as the Voronoï analysis requires individual particles to be clearly identified from images.[8]

It is worth pointing out here that the study of degree distributions and the concept of using the maximum shortest path length have also been used previously to study graphs. One example is the seminal work by the authors of Ref. 13 where degree distributions were used to study graphs, which model the Web, and the maximum shortest path length, referred to as the diameter of the graph, was used to study connected components.

Graph theory is now demonstrated on 2D experimental data acquired by particle image velocimetry, obtained from a confined counter-flow/jet system. The jet flow was seeded with inertial 80 μm sized spherical particles of density, 1050 Kg m^{-3}. The Reynolds number of a single phase gas jet with the same flow conditions as used in the experiment, based on the nozzle exit conditions, is about 4460. The Reynolds number of the single phase counter-flow without the jet present, based on the area-averaged velocity, is about 2192. The measurements were obtained at the stagnation region of the gas flow, located at about 21.4D$_{JET}$ from the nozzle of the jet, where D$_{JET}$ is the diameter of the nozzle. The Stokes number of the particles is 4.64, based on an estimated Kolmogorov scale of the jet at this location. The volume fraction is about 5.5×10^{-5}. Further details about the experiment are found in Ref. 14. Voronoï analysis was carried out on a sample of 1000 images each about 45×45 mm^2 in size. The total number of clusters identified from all images was $\mathcal{O}(7000)$. The present paper and subsequent figures focus only on data collected from the same experiment system and conditions as described above.

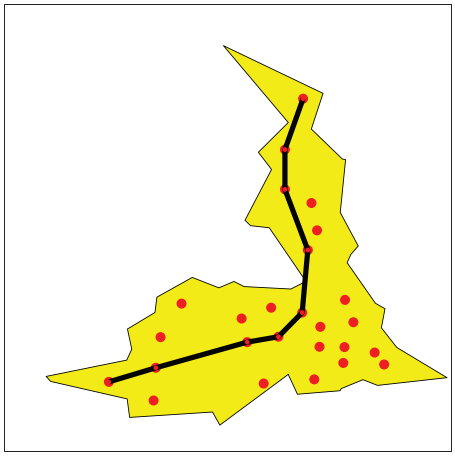


FIG. 4. An example of producing an approximate skeleton-like structure of a cluster identified from Voronoï analysis. The single (black) line is the maximum shortest path of the weighted graph between any two particles in the cluster. The weight used for each edge is the distance between the positions of the particles, denoted by $d_{i,j}$.

The degree of each node is calculated from the weighted graphs of each cluster containing exactly n = 10, 20, 30, or 40 particles. For each cluster, the mean and the skewness from the distribution of the degrees are then obtained and plotted against the square root area of the cluster, $\sqrt{\mathcal{C}_\mathcal{A}}$, nondimensionalized by the Kolmogorov scale, η. This is shown in Figs. 5 and 6, respectively.

For clusters with a fixed number of particles, the mean degree of the cluster reduces with increasing cluster size (Fig. 5). This suggests that larger clusters of the same number of particles typically have fewer number of collision pairs. Within the range of cluster particle sizes explored, this effect appears to be independent of the number of particles contained in the cluster. If the number of particles is kept the same, as the size of the cluster increases, intuitively the distance between the particles must also increase. This corresponds to the reduction observed in the mean degree, which may lead to fewer number of collision pairs. There is significant scatter present in Fig. 6, with values of both positive and negative skewness observed, suggesting a nonrandom particle distribution within the cluster. A positive skewness suggests that particular areas within the cluster have a higher local collision probability. A negative skewness suggests that particular areas within the cluster have a lower local collision probability, as they have a small number of neighbors. This may represent particles, which are on the periphery of the cluster boundary, such as $\mathcal{Z}_1$ in Fig. 2.

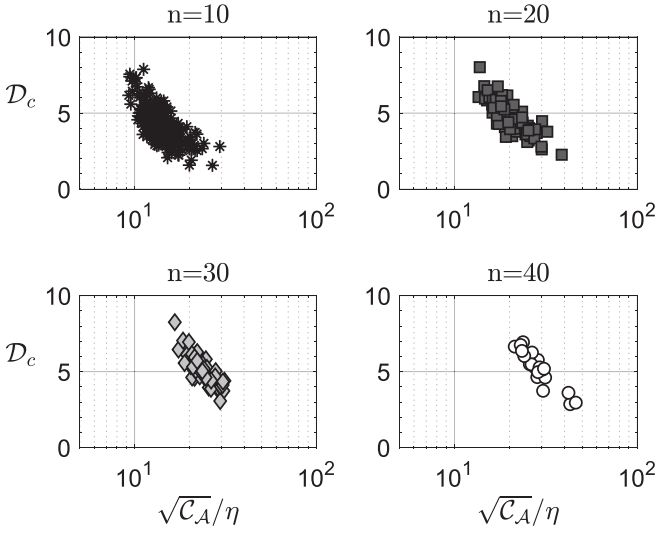


FIG. 5. A plot of the mean degree for a weighted graph of the cluster, $\mathcal{D}_c$, against the nondimensionalized square root of the area of the cluster, $\frac{\sqrt{\mathcal{C}_\mathcal{A}}}{\eta}$, obtained from the Voronoï analysis. The Kolmogorov scale of the surrounding flow is estimated for flow conditions in a single-phase jet and is denoted by η. The weight used for each edge is the inverse distance between the positions of the particles, denoted by $\frac{1}{d_{i,j}}$.

26 March 2024 16:31:13

Published under an exclusive license by AIP Publishing

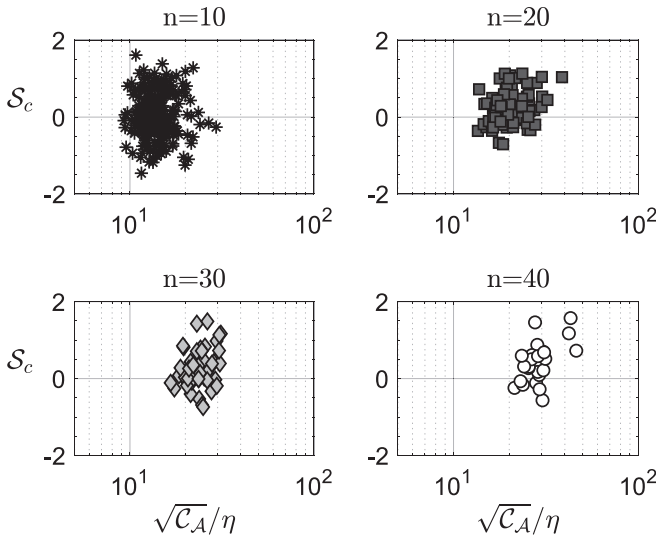


FIG. 6. A plot of the skewness of the distribution of the degree for a weighted graph of the cluster, $\mathcal{S}_c$, against the nondimensionalized square root of the area of the cluster, $\frac{\sqrt{\mathcal{C}_\mathcal{A}}}{\eta}$, obtained from the Voronoï analysis. The Kolmogorov scale of the surrounding flow is estimated for flow conditions in a single-phase jet and is denoted by η. The weight used for each edge is the inverse distance between the positions of the particles, denoted by $\frac{1}{d_{i,j}}$.

It is important to note that the Voronoï analysis and subsequent cluster identification are based on the area of the cells, compared to a threshold area. Sometimes, a Voronoï cell that falls below the threshold area is determined to comprise a cluster, but the position of the particle inside this cell is quite far from the other particles in the cluster. This is shown for the particle labeled 69 in Fig. 7 and for the particles around the hole on the top left of the figure. This is addressed by graph theory using a weight on the edges based on distance. In this case, the weight is $\frac{1}{d_{i,j}}$, since the objective is to increase the edge weight as the distance between the particles decreases.

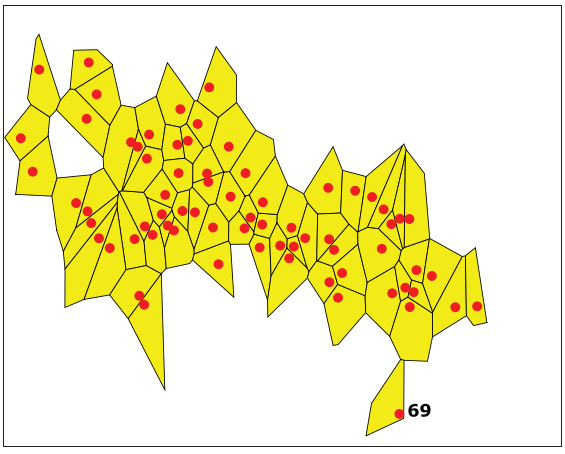


FIG. 7. The particle labeled 69 is far from all other particles inside the cluster, but it is still considered part of the cluster since its corresponding Voronoï cell falls below the area threshold.

In Fig. 6, the clusters with a higher fixed number of particles are typically larger in size. As the number of particles inside the clusters increases, the skewness values appear to become more positive. This is shown more clearly in Fig. 8 for the histograms of the skewness values, conditioned on clusters containing n = 10, 20, 30, or 40 particles. Clusters containing a higher fixed number of particles are therefore more likely to have concentrated regions of particles.

Next, the maximum shortest path length for the weighted graph of each cluster is calculated, for all cluster sizes. In this case, the weighting used for each edge is $d_{i,j}$. Figure 9 shows a histogram of the values and indicates that the characteristic length scale of the clusters, as determined from the mode of this data set, is $\mathcal{O}(10\eta)$. This is half the predicted length scale using box counting, which was found to be $\mathcal{O}(20\eta)$.[14] The discrepancy can be attributed to the inflexible rectangular shape of the sampling boxes in the box counting method, which are not able to accommodate the fractal-like shape of the clusters.

A feature in the proposed method that distinguishes it from skeletonization is that it provides an estimate of the cluster length along an unbranched line, capturing the main body of the cluster. Skeletonization produces a series of smaller lines, which can deviate from the main body of the cluster. It is desirable to only have a single line when estimating the characteristic length scale of clusters. This is because the length of any branches is not relevant to the cluster length scale. The proposed method is however complementary and not a replacement for skeletonization as it may not be ideal for clusters that bifurcate significantly or contain large holes. It is also possible that the path line may sometimes cross the boundaries of the cluster, as shown in Fig. 4, but such deviations are small and unlikely to have an appreciable effect on the evaluation of the cluster length scale.

One aspect of clusters readily observed is that they come in a wide range of complex shapes and sizes, which has previously been described as fractal-like.[3,15] The characteristic length scale estimated by the maximum shortest path length in the present paper, $\mathcal{O}(10\eta)$, is

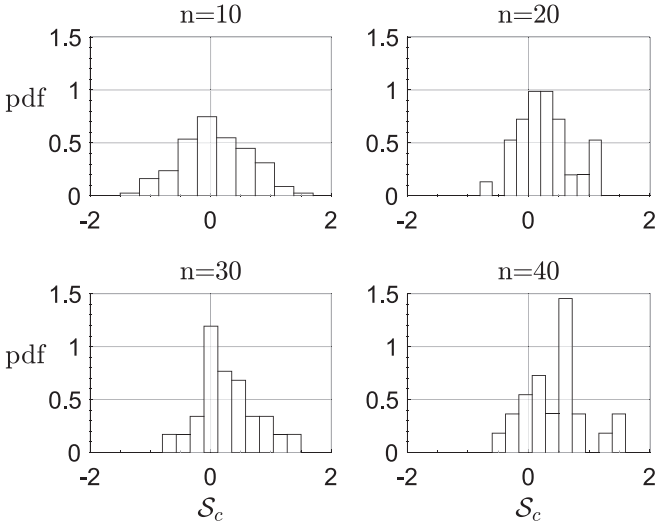


FIG. 8. A probability density function (PDF), of the skewness values shown in Fig. 6. For each sub-figure, the range of skewness values, $\mathcal{S}_c$, are sub-divided into 10 bins; however, a similar result is also observed if an automated binning method (with arbitrary number of bins) is used instead.

26 March 2024 16:31:13

Published under an exclusive license by AIP Publishing

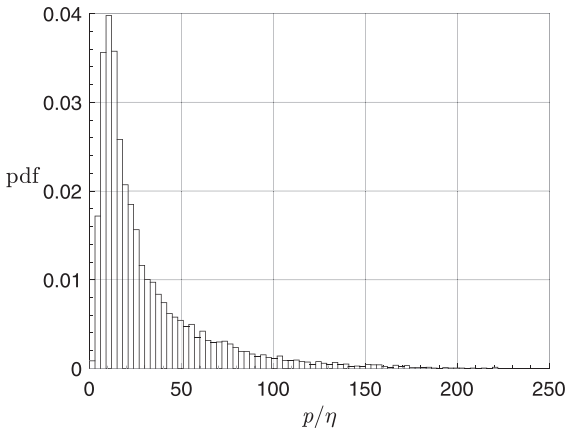


FIG. 9. A probability density function (PDF), of the maximum shortest path length p of each cluster $\mathcal{C}_k$ for weighted graphs, normalized by the estimated Kolmogorov scale. The weighting used for each edge is $d_{i,j}$.

in the range of values found in previous studies.[3,15] Using the mean and skewness of the distribution of degrees of the network graphs, the present work also hints at a complex sub-structure inside the clusters. Consider now the group of clusters which contain an exact number of particles. An averaged cluster square root area, $\langle \frac{\sqrt{\mathcal{C}_A}}{\eta} \rangle$, can be obtained by summation of the areas in the group followed with division by its total number [Fig. 10(a)]. Similarly, an averaged mean degree, $\langle \mathcal{D}_c \rangle$ [Fig. 10(b)] and averaged skewness degree, $\langle \mathcal{S}_c \rangle$ [Fig. 10(c)], can be obtained. As the size of the cluster increases, it appears that three effects occur: (i) increased number of particles, which comprise the cluster [Fig. 10(a)]; (ii) a lower mean value for the distribution of degrees (Fig. 5); and (iii) a higher skewness value for the distribution of degrees [Fig. 10(c)].

These three effects provide physical insight into how different sized and populated clusters influence collision pairs, therefore promoting particle collisions. For clusters comprised of a fixed number of particles, a wide range of cluster shapes and sizes exist, with larger cluster sizes less favorable as the number of collision pairs is reduced (Fig. 5). However, upon averaging out the effects of the different cluster sizes for each particle group, collision pairs were found to increase with large cluster sizes [Figs. 10(b) and 10(c)]. This suggests that internal structure exists within the cluster, which increases the collision probability and its affect is more profound on larger clusters.

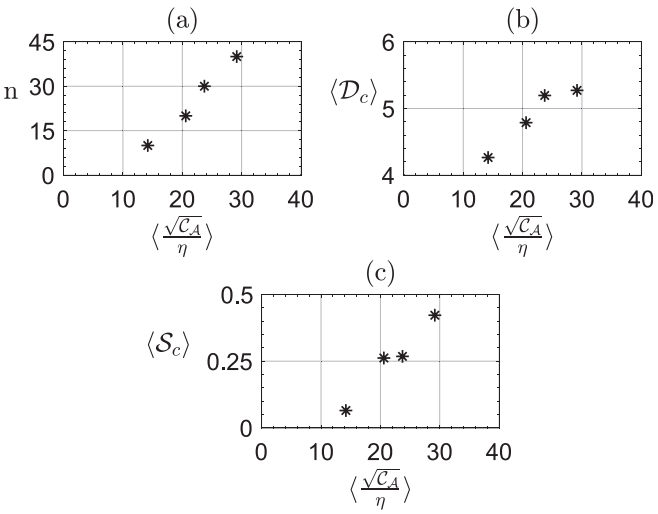


FIG. 10. Plots of particle number, which comprise a cluster (a), averaged mean degree (b), and averaged skewness (c) against the averaged normalized square root area.

In general, most particles that comprise a large cluster have few neighboring particles in comparison with a minority, which happen to be surrounded by a very large number of particles. The finding is similar to the idea of "coherent clusters,"[10,16] where sufficiently large clusters exhibit self-similarity, which means characteristics of the clusters remain scale independent. This is because positively skewed values suggest the particles in the large size clusters locally arrange themselves in a nonrandom way, similar to the particles preferentially concentrating in a nonrandom way in the entire flow domain. Conversely, the particles that comprise a small cluster are typically positioned randomly.

The behavior of both the mean and skewness of the degree of distributions, as well as the number particles that comprise the clusters, therefore reveals a complex picture of the influence of large or small size clusters in turbulent collision processes. It is noted here that these observations may be flow or location dependent. A future study that examines clusters formed in homogeneous isotropic turbulence would give insight into this issue.

One question to ask is whether the sub-structure is topologically equivalent. Study of the isomorphism property of two graphs may give insight into this issue. If a graph representing a cluster is found to be isomorphic with several other graphs representing other clusters, it may be that there exists a universal structural pattern to the cluster sub-structure. This requires a great number of clusters, with the same number of particles, to be observed and therefore is a tool more suited to numerical simulations at present.

Finally, one issue highlighted with the Voronoï analysis was that sometimes, a cell is included in a cluster where the particle which resides in it is far from other particles in the cluster, such as the case of particles of cells around cluster holes. This leaves some ambiguity about how to identify such cells if and when they occur and also whether to include them as part of the cluster. It is feasible that for each image domain, a single graph could be constructed and the degree of clustering, determined by a global clustering coefficient,[17] could describe the extent of the clustering. However, it is not easy to identify individual clusters from this single graph of all the particle positions. There also exists a possibility of using graph theory to track clusters in time. Graph theory was previously used to track the merging and splitting of coherent structures in single-phase turbulent flows,[18] and it has been suggested that this type of tracking may also be used for clusters.[19] However in Ref. 18, the nodes of the graph represent instead individual specific structures, which means a method is still needed beforehand to identify each cluster.

In conclusion, the Voronoï analysis technique to identify clusters in turbulent flows was extended using graph theory. This new approach provides additional insight into the internal structure of a cluster and a new way to measure its characteristic length scale. Additional tools also exist in graph theory, which may give further insight. The use of graph theory in the present paper requires Voronoï

26 March 2024 16:31:13

Published under an exclusive license by AIP Publishing

analysis, but there is scope to use it independently or with other techniques, which are capable of identifying clusters. The next step should therefore be to investigate further the new technique, with additional tools, on a wider range of other flow systems.

The authors acknowledge the support from the Engineering and Physical Sciences Research Council (EPSRC) through Grant No. EP/K019732/1. One of the authors was supported by an EPSRC industrial case studentship in collaboration with Procter & Gamble.

AUTHOR DECLARATIONS

Conflict of Interest

The authors have no conflicts to disclose.

DATA AVAILABILITY

The data that support the findings of this study are available from the corresponding author upon reasonable request.

REFERENCES

[1]P. A. Vaillancourt and M. K. Yau, "Review of particle-turbulence interactions and consequences for cloud physics," Bull. Am. Meteorol. Soc. **81**, 285 (2000).
[2]T. Langrish and D. Fletcher, "Spray drying of food ingredients and applications of CFD in spray drying," Chem. Eng. Process. **40**, 345 (2001).
[3]A. Aliseda, A. Cartellier, F. Hainaux, and J. C. Lasheras, "Effect of preferential concentration on the settling velocity of heavy particles in homogeneous isotropic turbulence," J. Fluid Mech. **468**, 77–105 (2002).
[4]M. Ernst, M. Sommerfeld, and S. Laín, "Quantification of preferential concentration of colliding particles in a homogeneous isotropic turbulent flow," Int. J. Multiphase Flow **117**, 163 (2019).
[5]S. Sundaram and L. R. Collins, "Collision statistics in an isotropic particle-laden turbulent suspension. Part 1. Direct numerical simulations," J. Fluid Mech. **335**, 75–109 (1997).
[6]J. R. Fessler, J. D. Kulick, and J. K. Eaton, "Preferential concentration of heavy particles in a turbulent channel flow," Phys. Fluids **6**, 3742 (1994).
[7]R. Monchaux, M. Bourgoin, and A. Cartellier, "Preferential concentration of heavy particles: A Voronoï analysis," Phys. Fluids **22**, 103304 (2010).
[8]T. C. Lau and G. J. Nathan, "A method for identifying and characterising particle clusters in a two-phase turbulent jet," Int. J. Multiphase Flow **88**, 191 (2017).
[9]J.-S. Ferenc and Z. Néda, "On the size-distribution of Poisson Voronoi cells," Physica A **385**, 518 (2007).
[10]L. Baker, A. Frankel, A. Mani, and F. Coletti, "Coherent clusters of inertial particles in homogeneous turbulence," J. Fluid Mech. **833**, 364–398 (2017).
[11]T. H. Cormen, C. E. Leiserson, R. L. Rivest, and C. Stein, *Introduction to Algorithms* (MIT Press, 2001).
[12]M. Manish and S. Sahu, "Analysis of droplet clustering in air-assist sprays using Voronoi tessellations," Phys. Fluids **30**, 123305 (2018).
[13]A. Broder, R. Kumar, F. Maghoul, P. Raghavan, S. Rajagopalan, R. Stata, A. Tomkins, and J. Wiener, "Graph structure in the web," Comput. Networks **33**, 309 (2000).
[14]P. Andrade, "Interaction of particles, droplets and turbulent gas flow and consequences for spray drying," Ph.D. thesis (Imperial College London, 2019).
[15]M. Obligado, T. Teitelbaum, A. Cartellier, P. Mininni, and M. Bourgoin, "Preferential concentration of heavy particles in turbulence," J. Turbul. **15**, 293 (2014).
[16]A. J. Petersen, L. Baker, and F. Coletti, "Experimental study of inertial particles clustering and settling in homogeneous turbulence," J. Fluid Mech. **864**, 925–970 (2019).
[17]M. E. J. Newman, "Clustering and preferential attachment in growing networks," Phys. Rev. E **64**, 025102 (2001).
[18]A. Lozano-Durán and J. Jiménez, "Time-resolved evolution of coherent structures in turbulent channels: Characterization of eddies and cascades," J. Fluid Mech. **759**, 432–471 (2014).
[19]Y. Liu, L. Shen, R. Zamansky, and F. Coletti, "Life and death of inertial particle clusters in turbulence," J. Fluid Mech. **902**, R1 (2020).

26 March 2024 16:31:13

Published under an exclusive license by AIP Publishing